Applied Physics Letters ARTICLE scitation.org/journal/apl

Band structure and ultraviolet optical transitions in ErN

Cite as: Appl. Phys. Lett. **118**, 131108 (2021); doi: 10.1063/5.0046580
Submitted: 4 February 2021 · Accepted: 15 March 2021 ·
Published Online: 30 March 2021

M. A. McKay,[1] H. A. Al-Atabi,[2,3] J. Li,[1] J. H. Edgar,[2] J. Y. Lin,[1] and H. X. Jiang[1,a)]

AFFILIATIONS

[1]Department of Electrical and Computer Engineering, Texas Tech University, Lubbock, Texas 79409, USA
[2]Tim Taylor Department of Chemical Engineering, Kansas State University, Manhattan, Kansas 66506, USA
[3]Chemical Engineering Department, the University of Technology, PO Box 35010 Baghdad, Iraq

[a)]**Author to whom correspondence should be addressed:** hx.jiang@ttu.edu

ABSTRACT

Erbium nitride (ErN) is a rare-earth metal mononitride continuing to receive interest due to its unique electronic, magnetic, and optical properties. ErN has shown promise in the development of new functional materials for optoelectronic and spintronic devices. Here, we report on the optical properties of ErN crystals, grown by sublimation and probed by photoluminescence (PL) spectroscopy at both room temperature and 180 K. Multiple transition lines were observed between 2 and 4.5 eV. Using the PL results together with reported calculations, a coherent picture for the band structure at the Γ-point for ErN crystals was derived. PL results revealed that ErN has a minimum direct energy gap of 2.41 eV and a total of two valence bands and two conduction bands at the Γ-point separated by about 0.15 eV and 0.34 eV, respectively. These transitions reveal optical properties of ErN in the UV region and its band structure at the Γ-point.

Interest in rare-earth nitrides (RENs) has been increasing recently due to their unique electronic, magnetic, and optical properties. Due to being the only stable elements with more than marginally filled f-shell electronic orbitals, they hold the largest spin and orbital moments.[1] Having the same crystalline structure and similar lattice constants, research into RENs has grown rapidly, motivated by materials demand with the emergence of spintronic devices.[1–6] RENs display a broad range of behavior, from metallic or semi-metallic to semiconducting.[7] With a valence band maximum (VBM) at the Γ-point and a conduction band minimum (CBM) at the X-point, their narrow minimum direct bandgaps (around 1 eV) and indirect bandgaps on the order of one half of that are useful for a variety of applications for infrared (IR) photonic devices.[2,8] Moreover, their semiconducting and ferromagnetic properties allow the spins of charge carriers to be exploited for fundamental studies and device applications.[1] Epitaxial growth of RENs is further motivated by the potential to be incorporated into III-nitride semiconductors to develop new optical devices because their temperature-stable luminescence wavelength is nearly independent of the specific semiconductor host.[9] Additionally, III-nitride and REN heterojunctions could also have desirable features for multiwavelength photonic devices.[10,11]

One of these RENs is erbium nitride (ErN), which has more than a half-filled 4f electron shell. ErN forms predominantly in the rock salt phase crystalline structure (like NaCl) with a lattice constant of 4.79 Å.[12] It has gained increasing attention in recent years due to its potential for diverse applications. Theoretical studies predict that ErN is a semi-metal in its ferromagnetic (FM) phase,[13–15] that it is a tough material (toughness/fracture ratio = 0.61), and that it possesses anisotropic thermal conductivity.[16] Simulations have shown that ErN has a small indirect energy gap of around 0.2 eV with a CBM at the X-point of the Brillouin zone and a VBM at the Γ-point. Experimentally, the smallest direct energy gap is 0.98 eV at the X-point, indicating possible applications for IR photonic devices.[8]

Erbium (Er) ions in wide bandgap semiconductors have also been extensively studied, both theoretically and experimentally, for their promising applications in areas such as solid-state lasers, optical amplifiers, and optoelectronic devices operating at the retina-safe and fiber optical communication wavelength window of 1.54 μm.[17–43] This is beneficial because it coincides with the wavelength of minimum optical loss in silica-based optical fibers. The emission lines near 1.54 μm in Er-doped GaN (Er:GaN) are due to the 4*f* intra-subshell transitions from the first excited state ($^4I_{13/2}$) to the ground state ($^4I_{15/2}$), of the Er trivalent ions (Er^{3+}). Erbium doped III-nitrides are very stable with a small thermal quenching effect[25,26,36,37,41,44–47] due to its large bandgap semiconductor hosts.[25] Er ions can be incorporated into thin Er:GaN epitaxial films at concentrations as high as

1%–2% with small thermal quenching.[26] However, several barriers have hindered Er:GaN applications as a robust optical gain medium for high energy lasers.[36–39] Because Er atoms are larger than Ga atoms, incorporating Er onto Ga lattice sites in GaN introduces strains and point defects into Er:GaN. Additionally, a phase transition from the wurtzite to rock salt crystal structure is expected for Er:GaN when the Er concentration surpasses a critical value since GaN and ErN have different crystalline structures. Therefore, understanding the optical transitions and the band structure of pure ErN can be helpful for controlling the basic growth processes and properties of Er:GaN gain materials, by identifying ErN domains in Er:GaN, and for potential applications of ErN.

Despite the numerous binary rare-earth nitride studies in the past decade, many of their fundamental properties have not been experimentally measured, particularly their optical properties. For example, the energy band structures are still not well established, including the energy bandgaps and the detailed valence and conduction band structures. In fact, experimentally determined optical transitions in the UV wavelengths have not been reported for REN materials, apart from transmission/reflectivity measurements on DyN.[48] In this work, we report the properties of the UV optical transitions in ErN, which were probed by photoluminescence (PL) spectroscopy at both room temperature and 180 K. By comparing our experimental results with theoretical calculations of the band structures,[2,12,13,15] we present a coherent picture for the band structure and optical transitions of ErN near the Γ-point of the Brillouin zone.

The ErN crystals were grown by the sublimation-recondensation method in a tungsten furnace heated by a resistive heater via a process that was previously described.[49,50] Because of the high temperature of this process (above the melting temperature of silicon), the ErN crystals were grown unseeded on a polycrystalline tungsten foil, which had predominately (100) textures.[50] First, this foil was cleaned sequentially by acetone, methanol, and isopropyl. The ErN source was synthesized by heating small chunks of Er metal (99% purity) in ultra-high-purity nitrogen at 1500 °C and 400 Torr for 15 h. The distance between the ErN source and the tungsten foil substrate was kept constant at approximately 2 cm. The ErN crystal growth was carried out in 1790 °C under a nitrogen pressure of 150 Torr. Growing the material at temperatures significantly higher than most epitaxial growth techniques (<1100 °C) produces much higher crystalline quality because it is closer to thermal equilibrium and produces higher adatom diffusivities, and diatomic nitrogen is more reactive.[50] To avoid the room temperature reaction with water vapor in ambient air that decomposes ErN to erbium oxide,[50] following crystal growth, the ErN sample was immediately sealed in argon jars with desiccant. The PL spectroscopy system used consists of a Coherent COMPex Pro 193 nm (6.42 eV) excimer laser and an Ocean Optics USB2000+ UV spectrometer.

Figure 1 shows an optical microscope image illustrating the preferential nucleation of ErN crystals at the tungsten foil's grain boundaries, which revealed that ErN tends to have 3D growth and does not form a thin film for short growth times. ErN adopted a predominately (100) orientation matching the predominant orientation of the tungsten foil.[50] The dark color represents the ErN crystals with average dimensions of $10 \times 5 \times 10\ \mu$m.

The PL spectroscopy measurements were conducted immediately following the opening of the sample container and exposure to the air. Figure 2 shows the measured PL spectrum for ErN at room temperature covering the energy range from 1.5 to 5 eV. Many emission lines

FIG. 1. Microscope image of the ErN crystals grown on the tungsten substrate at 1790 °C. The crystals adopted a predominately (100) orientation due to nucleation on the substrate's grain boundaries. The dark color represents the ErN crystals with average dimensions of $10 \times 5 \times 5\ \mu$m.

were resolved, with their peak positions indicated on the graph. The large intensities of the 2.35, 2.54, 2.75, 2.90, 3.41, 4.15, and 4.32 eV peaks may be due to the band-to-band transitions. The smaller intensities of 3.26, 3.66, and 3.81 eV peaks suggest impurities or that the sample has begun to oxidize. The very narrow linewidth of the 3.41 eV peak indicates a possibility of transition from other high symmetry points other than that at the Γ-point.

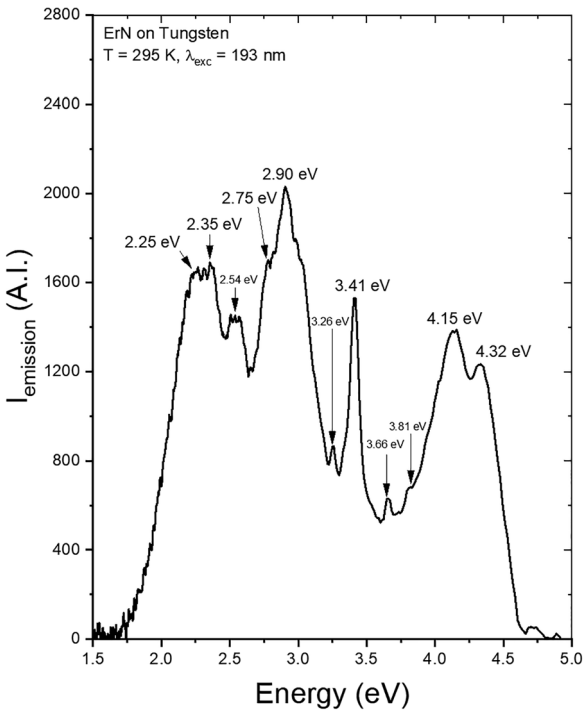

FIG. 2. Photoluminescence spectrum of ErN measured at room temperature with the above-bandgap 6.42 eV ($\lambda = 193$ nm) excitation energy. The arrows indicate the energy positions of the dominant transition peaks.

Immediately following the room temperature PL spectroscopy measurement, the sample was placed on an Al block, which was then partially submerged in liquid nitrogen, and a thermocouple was used to record the temperature. The PL spectroscopy measurement was then re-performed. The emission spectrum at 180 K is shown in Fig. 3. Six emission lines were observed. Here, the 2.40, 2.56, 2.75, and 2.90 eV peak intensities are significantly higher than those at higher temperature as shown in Fig. 2, similar to most semiconductors. The energy positions of these peaks suggest that these transitions are due to a two two-level system with separations of 0.15 and 0.34 eV. The 4.19 and 4.36 eV peaks decreased in intensity at higher temperature, but the other peaks (3.41, 3.26, 3.66, and 3.81 eV) either decreased in intensity significantly or became outweighed by the tails of other peaks and resulted in very weak emission lines. This is expected since occupation of charge carriers in the higher energy levels of bands decreases as temperature increases due to the Boltzmann distribution. The 2.56, 2.75, and 2.90 peaks are clearly very sharp with a narrow linewidth, but the linewidths of the 4.19 and 4.36 eV peaks appear to have increased at lower temperatures.

The band structure of ErN was previously calculated using various methods.[2,11,12,14] The electronic structures predicted by these different methods were not consistent, and they were focused on the magnetic properties of ErN. There has been no conclusion on the values of the minimum direct energy bandgap at the Γ-point. However, calculations have concluded that there are a total of two valence bands and two conduction bands at the Γ-point, which can contribute to the band-to-band transitions with an emission energy of around 2.65 eV between the lowest conduction band (B-CB) and the highest valence band or the minimum direct energy bandgap at the Γ-point. The calculated energy separation between the two lowest valence bands at the Γ-point is disputed and ranges from 0 to 0.5 eV, depending on the type of calculation. The energy separation between the first and second conduction band (A-CB) ranges from 0 to 0.72 eV, also depending on the type of calculation.[2,12,13,15]

By matching the energy positions of the four main emission peaks between 2.41 and 2.90 eV in our PL results with the calculated band structures of ErN,[2,12,13,15] the band structure at the Γ-point can, thus, be deduced and is shown in Fig. 4. Our PL results shown in Figs. 2 and 3, together with calculations,[2,12,13,15] suggest that the minimum direct energy bandgap at the Γ-point is 2.41 eV. The peaks at 2.56, 2.75, and 2.90 eV were also attributed to the band-to-band transitions at the Γ-point, due to their significantly higher intensity in Fig. 3. Our PL results show that the energy separation, at the Γ-point, between the two lowest valence bands is 2.56–2.41 = 0.15 eV and the energy separation between the A- and B-conduction bands is 2.75–2.41 = 0.34 eV.

The cause of other peaks shown in Figs. 2 and 3 could not be fully identified. The peak below 2.3 eV is likely due to the formation of Er_2O_3.[51] The three higher intensity peaks above 3.2 eV (3.41, 4.15, and 4.32 eV) are possibly due to band-to-band transitions at the K-point.[15] The other three lower intensity peaks above 3.2 eV (3.26, 3.66, and 3.81 eV) are possibly the result of impurities or the presence of Er_2O_3 due to air exposure.[51] Note that oxygen in ErN is a donor. We assume that the concentration of impurities and defects in this case is sufficiently low and that they do not affect the band structure of ErN. Thus, our proposed band structure of ErN will not be affected by the presence of oxygen impurities. We believe that our experimental results provide useful insight for further improving the calculation results of the band structure of ErN.

In conclusion, we have conducted sublimation growth and PL spectroscopy studies of ErN at low and room temperatures. Many emission lines between 1.5 and 5 eV were observed. Four of these emission lines are assigned to the band-to-band transitions at the

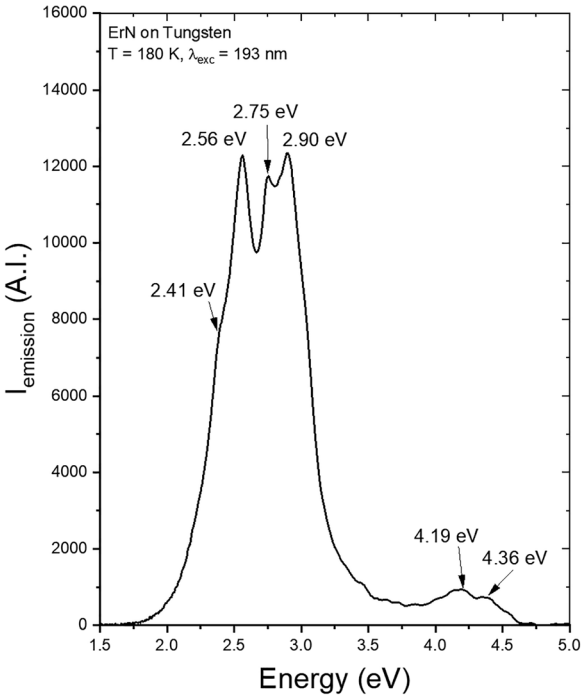

FIG. 3. PL spectrum measured at 180 K with the above-bandgap 6.42 eV (λ = 193 nm) excitation energy. The arrows indicate the energy positions of the dominant transition peaks.

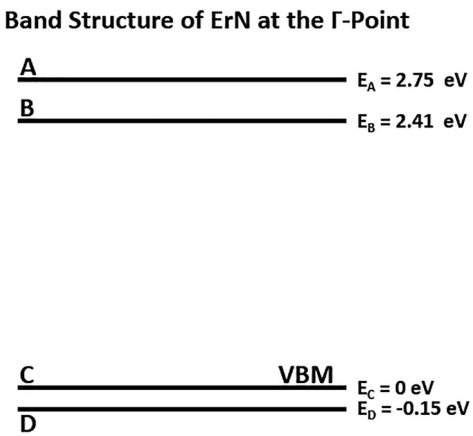

FIG. 4. The proposed band structure of ErN near the Γ-point of the Brillouin zone that was derived from the measured PL spectra together with calculated electronic band structures (Refs. 2, 12, 13, and 15). The minimum direct bandgap of ErN at the Γ-point, determined from PL spectra, is 2.41 eV other than 2.65 eV based on calculation results of (Ref. 2).

Γ-point. By combining the previously published theoretical band structures and PL spectroscopic results of ErN, we presented a more detailed understanding for the band structure near the Γ-point and the associated optical transitions in ErN. The PL spectroscopic results at both room and low temperatures and the subsequent detailed band structure will also help to further understand the basic properties and practical applications in the UV and multiwavelength photonic devices of this unique and less understood material.

H. X. Jiang and J. Y. Lin would like to acknowledge the support of Whitacre Endowed Chairs by the AT&T Foundation. Support for the ErN crystal growth was provided by the National Science Foundation Division of Materials Research (Award No. 1508172) and Higher Committee for Education Development in Iraq.

DATA AVAILABILITY

The data that support the findings of this study are available within this article.

REFERENCES

[1]F. Natali, B. J. Ruck, N. O. V. Plank, H. J. Trodahl, S. Granville, C. Meyer, and W. R. L. Lambrecht, Prog. Mater. Sci. **58**, 1316 (2013).
[2]P. Larson, W. R. L. Lambrecht, A. Chantis, and M. V. Schilfgaarde, Phys. Rev. B. **75**, 045114 (2007).
[3]F. Natali, N. Plank, J. Galipaud, B. Ruck, H. Trodahl, F. Semond, S. Sorieul, and L. Hirsch, J. Cryst. Growth **312**, 3583 (2010).
[4]C. M. Aerts, P. Strange, M. Horne, W. M. Temmerman, Z. Szotek, and A. Svane, Phys. Rev. B **69**, 045115 (2004).
[5]M. Horne, P. Strange, W. M. Temmerman, Z. Szotek, A. Svane, and H. Winter, J. Phys.: Condens. Matter **16**, 5061 (2004).
[6]Z. Szotek, W. M. Temmerman, A. Svane, L. Petit, P. Strange, G. M. Stocks, D. Koddertitzsch, W. Hergert, and H. Winter, J. Phys.: Condens. Matter **16**, S5587 (2004).
[7]F. Hulliger, *Handbook on the Physics and Chemistry of Rare Earths* (Elseveir, Amsterdam, 1979), Vol. 17, p. 301.
[8]M. A. McKay, Q. W. Wang, H. A. Al-Atabi, Y. Q. Yan, J. Li, J. H. Edgar, J. Y. Lin, and H. X. Jiang, Appl. Phys. Lett. **116**, 171104 (2020).
[9]M. Thaik, U. Hömmerich, R. N. Schwartz, R. G. Wilson, and J. M. Zavada, Appl. Phys. Lett. **71**, 2641 (1997).
[10]T. Kent, J. Yang, L. Yang, M. Mills, and R. Myers, Appl. Phys. Lett. **100**, 152111 (2012).
[11]R. Dargis, R. Smith, F. E. Arkun, and A. Clark, Phys. Status Solidi C **11**, 569 (2014).
[12]S. Dergal, A. E. Merad, and B. N. Brahmi, AMJST **2**, 40 (2013).
[13]P. Pandit, V. Srivastava, M. Rajagopalan, and S. P. Sanyal, Physica B **405**, 2245 (2010).
[14]A. G. Petukhov, W. R. L. Lambrecht, and B. Segall, Phys. Rev. B **53**, 4324 (1996).
[15]C. G. Duan, R. F. Sabirianov, W. N. Mei, P. A. Dowben, S. S. Jaswal, and E. Y. Tsmbal, J. Phys.: Condens. Matter **19**, 315220 (2007).
[16]V. Bhalla and D. Singh, Indian J. Pure Appl. Phys. **54**, 40 (2016).
[17]W. Koechner, *Solid State Laser Engineering*, 3rd ed. (Springer, Berlin, 1992).
[18]W. J. Miniscalco, J. Lightwave. Technol. **9**, 234 (1991).
[19]H. Ennen, J. Schneider, G. Pomrenke, and A. Axmann, Appl. Phys. Lett. **43**, 943 (1983).
[20]H. Ennen, G. Pomrenke, A. Axmann, K. Eisele, W. Haydl, and J. Schneider, Appl. Phys. Lett. **46**, 381 (1985).
[21]P. Galtier, J. P. Pochelle, M. N. Charasse, B. deCremoux, J. P. Hirtz, B. Broussin, T. Benyattou, and G. Guillot, Appl. Phys. Lett. **55**, 2105 (1989).
[22]H. Isshiki, H. Kobayashi, S. Yugo, T. Kimura, and T. Ikoma, Jpn. J. Appl. Phys., Part 2 **30**, L225 (1991).
[23]J. Michel, J. L. Benton, R. F. Ferrante, D. C. Jacobson, D. J. Eaglesham, E. A. Fitzgerald, Y. H. Xie, J. M. Poate, and L. C. Kimerling, J. Appl. Phys. **70**, 2672 (1991).
[24]G. Franzo, F. Priolo, S. Coffa, A. Polman, and A. Carnera, Apply. Phys. Lett. **64**, 2235 (1994).
[25]P. N. Favennec, H. L'Haridon, M. Salvi, D. Moutonnet, and Y. Le Guillon, Electron. Lett. **25**, 718 (1989).
[26]C. Ugolini, N. Nepal, J. Y. Lin, H. X. Jiang, and J. M. Zavada, Appl. Phys. Lett. **89**, 151903 (2006).
[27]N. Ter-Gabrielyan, V. Fromzel, X. Mu, H. Meissner, and M. Dubinskii, Opt. Lett. **38**, 2431 (2013).
[28]J. O. White, IEEE J. Quantum Electron. **45**, 1213 (2009).
[29]M. Nemec, J. Sulc, L. Indra, M. Fibrich, and H. Jelınkova, Laser Phys. **25**, 015803 (2015).
[30]T. Sanamyan, J. Opt. Soc. Am. B **33**, D1 (2016).
[31]D. J. Ottaway, L. Harris, and P. J. Veitch, Opt. Express **24**, 15341 (2016).
[32]J. M. Zavada, S. X. Jin, N. Nepal, J. Y. Lin, H. X. Jiang, P. Chow, and B. Hertog, Appl. Phys. Lett. **84**, 1061 (2004).
[33]R. Dahal, C. Ugolini, J. Y. Lin, H. X. Jiang, and J. M. Zavada, Appl. Phys. Lett. **95**, 111109 (2009).
[34]R. Dahal, C. Ugolini, J. Y. Lin, H. X. Jiang, and J. M. Zavada, Appl. Phys. Lett. **97**, 141109 (2010).
[35]D. K. George, M. D. Hawkins, M. McLaren, H. X. Jiang, J. Y. Lin, J. M. Zavada, and N. Q. Vinh, Appl. Phys. Lett. **107**, 171105 (2015).
[36]Z. Y. Sun, J. Li, W. P. Zhao, J. Y. Lin, and H. X. Jiang, Appl. Phys. Lett. **109**, 052101 (2016).
[37]Z. Y. Sun, Q. W. Wang, J. Li, J. Y. Lin, and H. X. Jiang, Proc. SPIE **10528**, 105280E (2018).
[38]Y. Q. Yan, Z. Y. Sun, W. P. Zhao, J. Li, J. Y. Lin, and H. X. Jiang, Appl. Phys. Express **12**, 075505 (2019).
[39]Z. Y. Sun, Y. Q. Yan, T. B. Smith, W. P. Zhao, J. Li, J. Y. Lin, and H. X. Jiang, Appl. Phys. Lett. **114**, 222105 (2019).
[40]F. Iacona, D. Pacifici, A. Ierrera, M. Miritello, G. Franzo, F. Priolo, D. Sanfilippo, D. Stefano, and G. Fallica, Appl. Phys. Lett. **81**, 3242 (2002).
[41]Z. Y. Sun, Y. Q. Yan, W. P. Zhao, J. Li, J. Y. Lin, and H. X. Jiang, Appl. Phys. Lett. **112**, 202103 (2018).
[42]Z. Y. Sun, L. C. Tung, W. P. Zhao, J. Li, J. Y. Lin, and H. X. Jiang, Appl. Phys. Lett. **111**, 072109 (2017).
[43]D. W. Jeon, Z. Y. Sun, J. Li, J. Y. Lin, and H. X. Jiang, Opt. Mater. Express **5**, 596 (2015).
[44]R. G. Wilson, R. N. Schwartz, C. R. Abernathy, S. J. Pearton, N. Newman, M. Rubin, T. Fu, and J. M. Zavada, Appl. Phys. Lett. **65**, 992 (1994).
[45]R. Birkhahn, M. Garter, and A. J. Steckl, Appl. Phys. Lett. **74**, 2161 (1999).
[46]A. J. Steckl, J. C. Heikenfeld, D. S. Lee, M. J. Garter, C. C. Baker, Y. Q. Wang, and R. Jones, IEEE J. Sel. Top. Quantum Electron. **8**, 749 (2002).
[47]M. Stachowicz, A. Kozanecki, C. G. Ma, M. G. Brik, J. Y. Lin, H. X. Jiang, and J. M. Zavada, Opt. Mater. **37**, 165 (2014).
[48]M. Azeem, B. J. Ruck, B. D. Le, H. Warring, H. J. Trodah, N. M. Strickland, A. Koo, V. Goian, and S. Kamba, J. Appl. Phys. **113**, 205309 (2013).
[49]Z. Gu, J. H. Edgar, J. Pomeroy, M. Kuball, and D. Coffey, J. Mater. Sci. **15**, 555 (2004).
[50]H. A. Al-Atabi, Z. F. Al Auda, B. Padavala, M. Craig, K. Hohn, and J. H. Edgar, Cryst. Growth Des. **18**(7), 3762 (2018).
[51]E. Nogales, B. Méndez, J. Piqueras, R. Plugaru, A. Coraci, and J. A. García, J. Phys. D: Appl. Phys. **35**, 295 (2002).